A superarmored lobopodian from the Cambrian of China and early disparity in the evolution of Onychophora

Jie Yang[a], Javier Ortega-Hernández[b,1], Sylvain Gerber[b], Nicholas J. Butterfield[b], Jin-bo Hou[a], Tian Lan[a], and Xi-guang Zhang[a,1]

[a]Yunnan Key Laboratory for Paleobiology, Yunnan University, Kunming 650091, China; and [b]Department of Earth Sciences, University of Cambridge, Cambridge CB2 3EQ, United Kingdom

We describe *Collinsium ciliosum* from the early Cambrian Xiaoshiba Lagerstätte in South China, an armored lobopodian with a remarkable degree of limb differentiation including a pair of antenna-like appendages, six pairs of elongate setiferous limbs for suspension feeding, and nine pairs of clawed annulated legs with an anchoring function. *Collinsium* belongs to a highly derived clade of lobopodians within stem group Onychophora, distinguished by a substantial dorsal armature of supernumerary and biomineralized spines (Family Luolishaniidae). As demonstrated here, luolishaniids display the highest degree of limb specialization among Paleozoic lobopodians, constitute more than one-third of the overall morphological disparity of stem group Onychophora, and are substantially more disparate than crown group representatives. Despite having higher disparity and appendage complexity than other lobopodians and extant velvet worms, the specialized mode of life embodied by luolishaniids became extinct during the Early Paleozoic. *Collinsium* and other superarmored lobopodians exploited a unique paleoecological niche during the Cambrian explosion.

Collins' monster | Xiaoshiba Lagerstätte | Cambrian explosion | evolution | phylogeny

Onychophorans, or velvet worms, comprise a relatively small phylum (~180 species) of soft-bodied panarthropods constituting a minor component of modern rainforest ecosystems around the world (1). The overall organization of extant onychophorans is remarkably conserved (2), typified by a low morphological variability and homogeneous autoecologies as ambush predators of small invertebrates. An emerging fossil record, however, points to a substantially wider range of forms and habits during their early evolutionary history (3–8). Paleozoic lobopodians—a paraphyletic group of soft-bodied extinct organisms resembling worms with legs—occupy basal phylogenetic positions within the stem lineages of Onychophora, Tardigrada, and Euarthropoda (3, 6, 9), and thus offer critical insights about the early evolution and paleobiology of panarthropod phyla. Here, we describe the stem group onychophoran *Collinsium ciliosum*, a "superarmored" lobopodian with complex limbs, based on a large and exquisitely preserved population from the early Cambrian (Stage 3) Xiaoshiba Lagerstätte in South China (10, 11) (*SI Appendix*, Fig. S1).

Systematic Paleontology

Superphylum Panarthropoda, Phylum (Stem Group) Onychophora, Family Luolishaniidae (12).

Diagnosis. Armored lobopodians with thorn-shaped dorsal sclerites, arranged in odd-numbered sets of three or more per trunk appendage pair; sclerite sets irregularly spaced, with separation decreasing progressively toward the anterior and posterior ends of the body; anteriormost five or six trunk limb pairs slender with double rows of long setiform spines (emended from ref. 6).

Included taxa. *Collinsium ciliosum* gen. et sp. nov., early Cambrian Stage 3, Xiaoshiba; *Acinocricus stichus*, middle Cambrian

Stage 5 Spence Shale (5); *Luolishania longicruris* early Cambrian Stage 3, Chengjiang (6); Collins' monster, early Cambrian Stage 4, Emu Bay Shale (7), and middle Cambrian Stage 5, Burgess Shale (4).

Collinsium ciliosum gen. et sp. nov.

Etymology. Named after Desmond Collins, who discovered and first illustrated the eponymous fossil (4); *ciliosum* (Latin), hairy.
Type material. Holotype YLKP 12127 (Fig. 1*A*); paratypes YLKP 12128 (Fig. 2*A*) and YLKP 12129 (Figs. 1*D* and 2*D*). YLKP: Key Laboratory for Paleobiology, Yunnan University.
Referred material. An additional 26 topotype specimens (YKLP 12130–12155).
Locality and horizon. Xiaoshiba section, Kunming, Yunnan Province; Cambrian Stage 3 (local upper Qiongzhusian), lower portion of the Hongjingshao Formation (10, 11) (*SI Appendix*, Fig. S1). The horizon has also been verified by a similar fossil assemblage found from another section in Kunming (13).
Diagnosis. Armored lobopodian with six pairs of setulose anterior appendages and 15 biomineralized sclerite sets: first sclerite set represented by a single pair of short dorsolateral spines; sets 2–15 composed of five spines of variable length. Nine posterior walking legs with single terminal claws. Head with pair of

Significance

Paleozoic lobopodians constitute a diverse assemblage of worm-like organisms that are known from various exceptional fossil deposits and were among the earliest animals to develop skeletonized body parts for protection. Here, we describe *Collinsium ciliosum* gen. et sp. nov., an armored lobopodian from the early Cambrian Xiaoshiba Lagerstätte (South China). *Collinsium* belongs to an extinct clade of superarmored lobopodians characterized by supernumerary dorsal spines, and specialized limbs for filter feeding; collectively, these fossil taxa represent a well-defined group within the lineage leading to extant velvet worms (Onychophora). Despite their greater morphological variety and appendage complexity compared with other lobopodians and extant velvet worms, *Collinsium* and its close relatives embodied a unique, yet ultimately failed, autoecology during the Cambrian explosion.
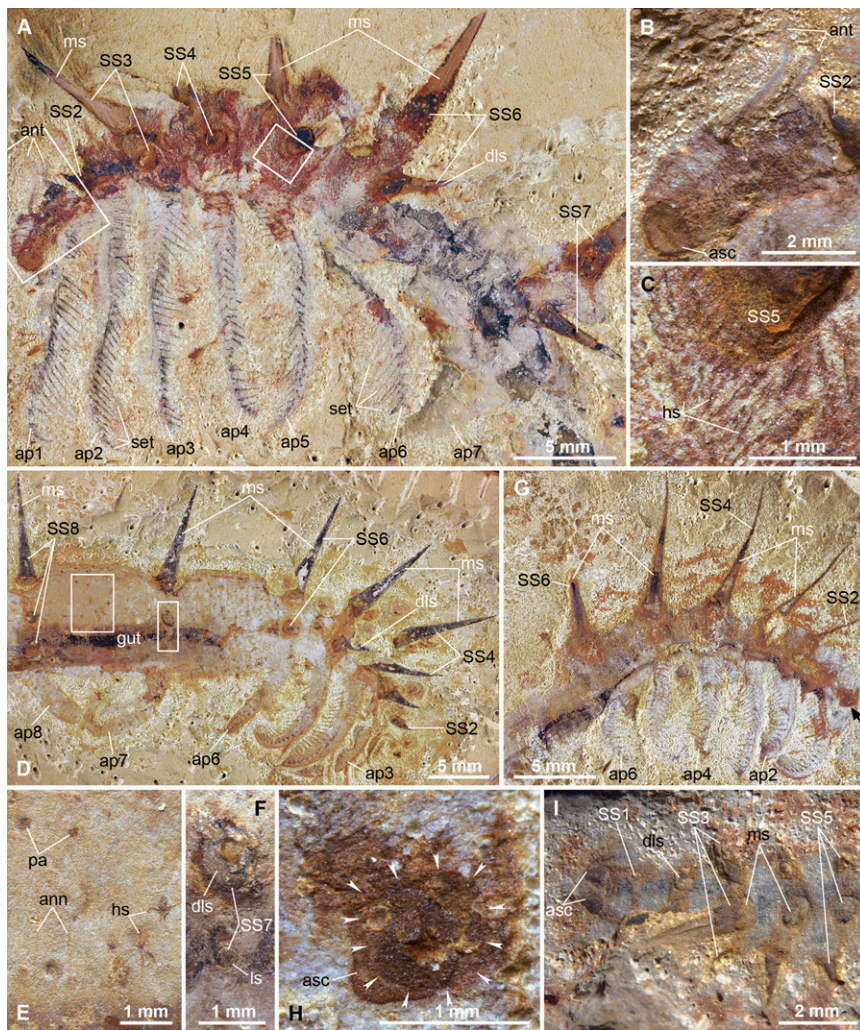
Fig. 1. Anterior morphology of *Collinsium ciliosum* from the early Cambrian (Stage 3) Xiaoshiba Lagerstätte. (*A–C*) YKLP 12127, holotype: (*A*) laterally preserved specimen, showing antenna-like limbs, six pairs of setiferous appendages, and limb correlation with sets of sclerotized dorsal spines; (*B*) detail of the head; (*C*) detail of the base of the fifth dorsal spine and short filiform setae. (*D–F*) YKLP 12129a, paratype: (*D*) lateral view showing correlation of appendages and sets of dorsal sclerotized spines; (*E*) details of the annulations, papillae, and fine hair-like setae; (*F*) bases of the dorsolateral spines and the lateral spines of the seventh sclerite set. (*G* and *H*) YKLP 12128, specimen with six pairs of setiferous appendages (arrowed): (*G*) lateral view; (*H*) detail of lateral overlap of the paired anterior sclerites on the head region; arrows indicate the outline of the left sclerite. (*I*) YKLP 12136, dorsal view showing organization of sclerite sets. Abbreviations: ann, annulations; ant, antennae; asc, anterior dorsal sclerites; dls, dorsal lateral spine; gut, digestive tract; hs, hair-like setae; ls, lateral spine; ms, medial spine; pa, papillae; set, setiform spines; SS1–15, sclerite series; tap1–15, appendages.

anterior antenna-like limbs and paired dorsal sclerites. Head and anterior trunk region densely covered by short filiform setae.

Description. Except for the three-dimensionally preserved dorsal spines, *Collinsium* specimens are preserved as flattened compression fossils. Complete individuals reach a maximum length of 85 mm. The elongate body is approximately tubular, widening gradually toward the middle section by a factor of ~1.5. The head region is bulbous, curves ventrally, and bears a terminal mouth lacking accessory oral structures (Fig. 1 *A*, *B*, and *G*, and *SI Appendix,* Fig. S3). A pair of subrectangular sclerotized plates converge dorsomedially on the head (Fig. 1 *B* and *G–I*), followed by a pair of anteriorly directed uniramous antenniform appendages (Fig. 1*B*); there is no evidence of eyes. The paired trunk limbs are uniramous and represented by two distinct morphotypes: the first to sixth pairs of trunk appendages are elongate (approximately one-third of the total body length), lack terminal claws or obvious annulations, and bear ~30 pairs of regularly spaced (~0.25 mm) 1.5- to 2.5-mm-long setiform spines that attach medially on the ventral side of the limbs to form a repeated chevron pattern (Figs. 1 *A* and *D*, and 2*A*, and *SI Appendix,* Fig. S4); by contrast, the 7th to 15th limb pairs are more conventionally lobopod-like with transverse epidermal annulations and a single terminal recurved claw that faces backward (Figs. 1*D* and 2 *A*, *C*, and *D*). The posterior end of the body terminates in a lobopodous extension beyond the last leg pair (*SI Appendix,* Fig. S6I).

Dorsolaterally, the trunk bears 15 metamerically arranged sets of three-dimensionally preserved sclerites (Figs. 1 *A*, *D*, *G*, and *I*,

and 2 *A*, *D*, and *E*, and *SI Appendix,* Figs. S5 and S6). Whereas the first sclerite set comprises a pair of short (<1-mm) dorsolateral spines (Fig. 1*I*), the 2nd to 15th sets consist of five spines, including the following: (*i*) a single, prominent, 6- to 12-mm-long medial spine; (*ii*) a pair of medium-sized (approximately one-third the length of the associated median spine) dorsolateral spines; and (*iii*) two smaller (approximately one-eighth the length of the associated median spine) lateral spines (Figs. 1 *A*, *C*, *D*, *F*, *G*, and *I*, and 2 *A*, *D*, and *E*). The distal portions of the spines curve gently toward the anterior (Figs. 1 *A*, *D*, and *G*, and 2*A*). The distance between sclerite sets and their respective ventral limb pairs decreases toward the anterior and posterior ends of the animal, such that sets 1–6 and 12–15 are separated by ~1–1.5 times the maximum width of the median spine, compared with a separation of ~3 times for sets 7–11 (Figs. 1 *A*, *D*, and *G*, and 2 *A* and *D*). The spines have subcircular bases, a punctate surface ornamentation, and a cone-in-cone construction similar to that described in hallucigeniids (3, 14, 15) (Figs. 1*C* and 2*G*). The three-dimensional preservation of the spines implies that they were originally biomineralized (16), and is supported by the cooccurrence of three-dimensionally preserved trilobites (*SI Appendix,* Fig. S1) (10). Elemental analysis of the spines reveals the presence of C and Fe, as well as selective depletion of Si, Al, and K, relative to the rock matrix (*SI Appendix,* Fig. S2); the taphonomically and geochemically indistinguishable preservation of *Microdictyon* sclerites from the adjacent—but stratigraphically older—Chengjiang deposits (14, 17) points to a
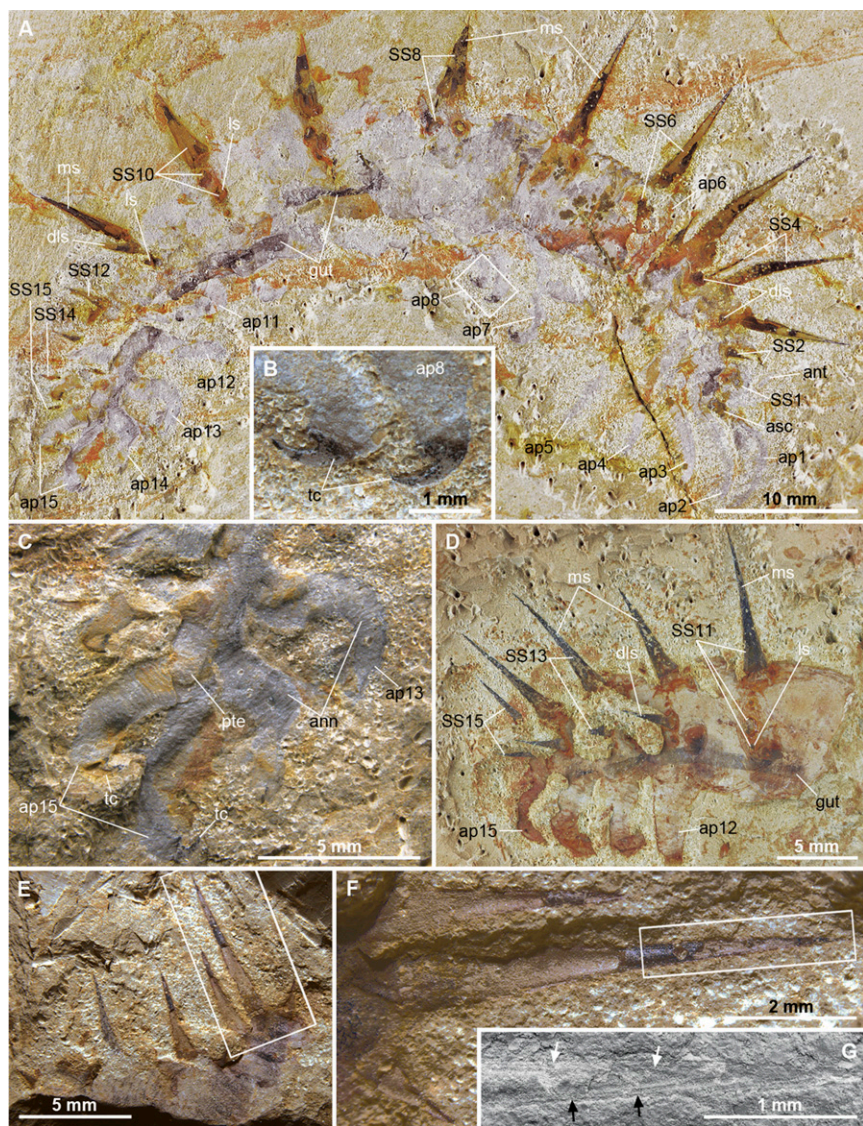
Fig. 2. Posterior morphology of *Collinsium ciliosum*. (*A–C*) YKLP 12149, paratype: (*A*) complete specimen in lateral view, showing 15 pairs of appendages and 15 sets of dorsal spines; (*B*) detail of terminal claws in posterior limbs; (*C*) detail of the most posterior portion of the trunk and appendages; (*D*) YKLP 12129b, showing the posteriormost dorsal spine sets and last four appendage pairs; (*E–G*) YKLP 12154, an incomplete specimen with well-preserved dorsal spines: (*E*) oblique dorsal view; (*F*) detail of three well-preserved spines in *E*; (*G*) SEM photomicrograph showing cone-in-cone construction of dorsal spines (marked in black and white arrows). Abbreviations: pte, posterior trunk extreme; tc, terminal claw; others as in Fig. 1.

similarly phosphatic composition for the original composition of *Collinsium* spines (15).

The trunk epidermis is marked by superficial annulations and is sparsely covered by small papillae (Figs. 1 *D–F* and 2 *C* and *D*). The anterior half of the body, including the head region to the sixth trunk appendage pair, is densely covered by short (~0.1- to 0.3-mm) hair-like setae (Fig. 1 *A* and *C*); slightly longer (~0.5-mm) filiform setae form a crown-like arrangement around the bases of the median and dorsolateral sclerotized spines (Fig. 1 *A* and *C*). The posterior half of the body appears to be devoid of hair-like setae, except for small bundles associated with papillae (Fig. 1*E*). The gut is the only internal structure preserved, represented by a simple flattened tube, ~1.5 mm in diameter, which follows the ventral curvature of the mouth (Figs. 1*D* and 2 *A* and *D*); there is no evidence for diverticulae or other specializations of the digestive tract.

Discussion

Although lobopodians are relatively well known from Cambrian Burgess Shale-type assemblages (3, 6–9, 14, 15), *Collinsium* differs from most representatives in its much more heavily developed dorsolateral armor and highly specialized anterior limbs (Figs. 1–3). Whereas other armored lobopodians are characterized by sclerite sets composed of a single pair of spines (e.g., hallucigeniids; refs. 12

and 14) or plates (e.g., *Microdictyon* and *Onychodictyon*; refs. 18–20) per appendage pair, the equivalent sclerite set in *Collinsium* consists of five variably sized biomineralized spines. The disposition of this dorsal covering would have presented an effective defensive barrier to potential predators, particularly if the constituent sclerites were capable of independent orientation (as suggested by the abundance of presumably sensory hair-like setae and papillae).
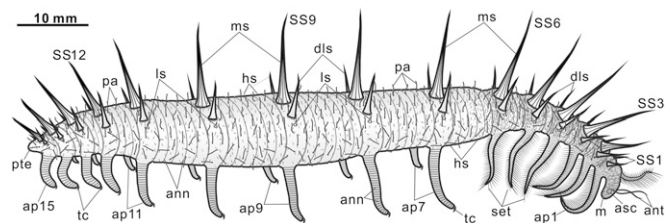

Fig. 3. Morphological reconstruction of *Collinsium ciliosum*. Abbreviations: ann, annulations; ant, antenna-like appendages; asc, anterior sclerite; dls, dorsolateral spines; hs, hair-like setae; ls, lateral spine; m, mouth; ms, medial spine; pa, papillae; pte, posterior trunk extension; set, setiform spines; SSn, sclerite series n; tap, trunk appendages; tc, terminal claw.
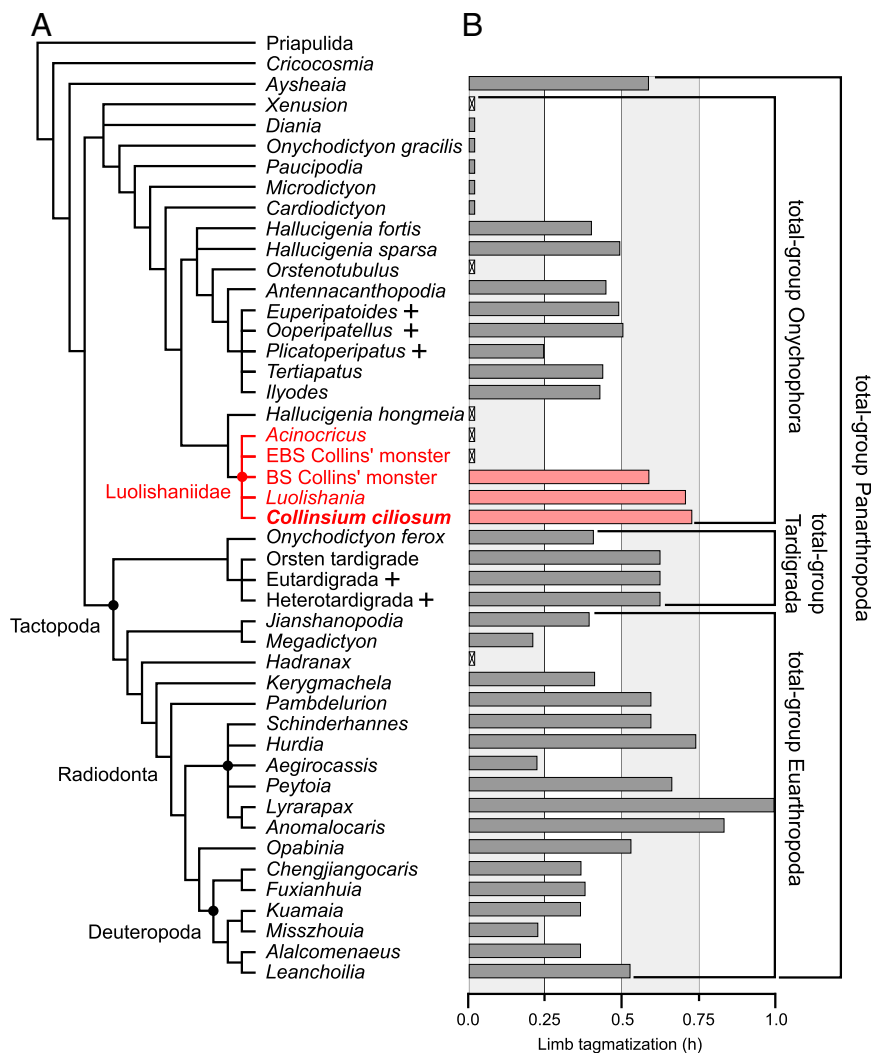
Fig. 4. Phylogeny and limb tagmosis of Paleozoic lobopodians. (A) Strict consensus of 123 most parsimonious trees (consistency index, 0.65; retention index, 0.87) under implied weights (k = 4); + denotes extant taxa. (B) Bar chart illustrating Brillouin index for appendage diversity (h) for each taxon (Dataset S1); crossed bars indicate insufficient data. Abbreviations: BS, Burgess Shale; EBS, Emu Bay Shale.

Given the accompanying absence of eyes or sclerotized oral/feeding structures, this emphasis on dorsal armor clearly rules out a macropredatory habit. Moreover, the batteries of closely spaced elongate setiform spines on the flexible anterior trunk appendages of *Collinsium* would have formed an efficient sieving basket (*SI Appendix*, Fig. S4), potentially deployed on flocculent organic-rich surface sediments (6). The well-developed terminal claws of the posterior legs, however, are poorly suited for walking on muddy substrates, suggesting instead a climbing or anchoring habit (6, 14, 21). Based on the putative association between other clawed lobopodians and sponges (22), *Collinsium* was most likely a benthic suspension feeder, favoring the higher energy conditions associated with hard substrates. Regardless of habitat preference, the derived feeding behavior of *Collinsium* must have exposed it to significantly greater levels of visual predation (23) than its less specialized relatives, hence its extraordinary investment in dorsal armor (Fig. 3).

Only a small subset of lobopodians shares with *Collinsium* the presence of setulose anterior limbs and supernumerary spines (i.e., more than one pair of spines per sclerite set) (*SI Appendix*, Fig. S7), most notably the enigmatic and as-yet-undescribed taxon informally referred to as the "Collins' monster" from the middle Cambrian Burgess Shale (4, 24). Known from just a single published specimen (4), the Collins' monster clearly bears a homologous row of long medial spines and anterior appendages with long setiform spines. Other documented taxa with a similar body organization—differing from *Collinsium* mainly in terms of

number of dorsal spines and leg pairs—include *Luolishania longicruris* from the early Cambrian Chengjiang biota (6), *Acinocricus stichus* from the middle Cambrian Spence Shale (5, 8), and a fragmentary specimen from the early Cambrian Emu Bay Shale (7). With the exception of *Collinsium* and *Luolishania*, however, most aspects of the morphology of these taxa are known from incomplete material, and evidence for spine biomineralization and cone-in-cone construction have only been demonstrated in the new taxon (Fig. 2G and *SI Appendix*, Fig. S2). A comprehensive phylogenetic analysis of Paleozoic lobopodians informed by developmental and paleoneurological data (Dataset S1 and *SI Appendix*, Notes S1 and S2) demonstrates that *Collinsium* and all other taxa with more than two dorsal spines per sclerite set and setulose anterior limbs form a well-defined clade of superarmored lobopodians—Family Luolishaniidae (6, 7, 12) (Fig. 4A and *SI Appendix*, Figs. S7 and S8). Luolishaniids, in turn, belong to a more inclusive group unified by posterior lobopodous legs with a single terminal claw and the variable length of the dorsal spines throughout the body. *Hallucigenia hongmeia* (14) occupies the most basal position within this latter clade, indicating the paraphyly of the genus *Hallucigenia*, or that the former species may merit a separate genus altogether. On a broader scale, luolishaniids are resolved as stem group representatives of Onychophora (per ref. 3; contra refs. 6 and 25), although these lobopodians fall outside of the direct lineage leading to crown group onychophorans (Fig. 4A). Insofar as
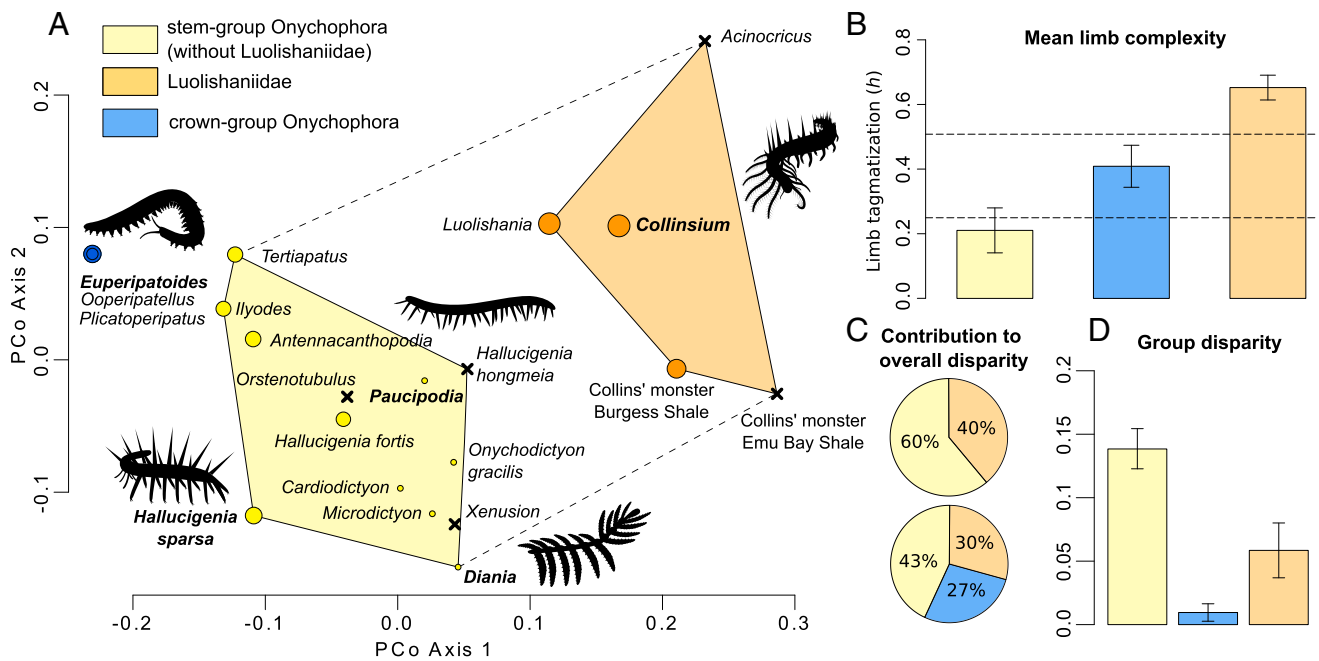
Fig. 5. Morphospace and disparity analyses of total-group Onychophora. (*A*) Visualization of the morphospace using a principal coordinate analysis. Circle size is proportional to the degree of limb complexity (Dataset S1 and Fig. 4*B*). X denotes unavailable or incomplete limb data for the taxon; dashed line indicates morphospace distribution for all members of stem group Onychophora. (*B*) Comparison of mean degree of limb complexity in stem and crown group Onychophora. Horizontal dashed lines outline the complete range of limb complexity observed in extant Onychophora (*SI Appendix*, Note S3, and Dataset S1). (*C*) Partial disparity analyses indicating the contribution to overall disparity of Luolishaniidae within stem group Onychophora (*Upper*) and within total-group Onychophora (*Lower*). (*D*) Comparison of group disparity in stem and crown group Onychophora.

luolishaniids exhibit a number of autapomorphic characters (e.g., specialized feeding limbs and supernumerary dorsal spines), they constitute a monophyletic group with no extant representatives (i.e., a plesion). Luolishaniids evince various morphological features that appear to be exclusive to total-group Onychophora in the wider context of panarthropod phylogeny; these include presence of a posterior extension of the lobopodous trunk, a dorsal armature consisting of metamerically arranged sets of sclerotized spines, the presence of stacked constituent elements (e.g., cone-in-cone dorsal spines), and the absence of a modified last pair of appendages (*SI Appendix*, Note S2) (3).

The strong support for luolishaniid monophyly revealed by the phylogenetic analysis (*SI Appendix*, Fig. S8 and Note S3) and the identification of these fossil organisms as members of stem group Onychophora are significant given the general scarcity of synapomorphic characters in Paleozoic lobopodians, which has led to controversy regarding their interrelationships and systematic classification (3, 6, 8, 9, 12, 14, 18–22). On a broader scale, these results illuminate large-scale morphological patterns during the early evolutionary history of Onychophora. The extraordinary degree of morphological differentiation in *Collinsium* and other luolishaniids—expressed in both dorsal armor and lobopodous appendage specialization (25, 26)—is unparalleled within total-group Onychophora. Although the limb complexity of crown group onychophorans surpasses that of most stem group representatives, luolishaniids possess by far the greatest degree of appendage tagmosis (Figs. 4*B* and 5*B*). Indeed, only highly derived nektonic predators within stem group Euarthropoda, such as some radiodontans (27, 28), display comparable levels. These observations evince parallel trends toward increasing overall limb complexity among lobopodians in the stem lineages of both Onychophora and Euarthropoda (Fig. 4*B*), possibly as a result of interspecific competition and ecological escalation in early Paleozoic ecosystems (29). Morphological analyses indicate that *Collinsium*

and its close relatives occupy a distinct and nonoverlapping region of morphospace compared with other total-group onychophorans (Fig. 5*A*). Despite being known from only five species—including *Collinsium*—and temporally restricted to early (6, 7) and middle Cambrian (4, 5) deposits, luolishaniids contribute 40% of the overall disparity of stem group Onychophora and 30% of the disparity observed in the total group (Fig. 5*C*); strikingly, the morphological disparity within Luolishaniidae is more than six times greater than that of crown group Onychophora (Fig. 5*D*). By contrast, extant onychophorans occupy a restricted distribution in morphospace (Fig. 5*A*) that largely reflects their conservative appendage construction—consisting of protocerebral "antennae," deutocerebral jaws, slime papillae, and a variable number of homonomous walking legs—as well as relatively low degrees of variation in other aspects of their nonappendicular morphology (2, 30) (Fig. 5 *B* and *D*). Our analyses of *Collinsium* and other luolishaniids indicate that the early evolutionary history of Onychophora was typified by exceptionally high levels of morphological and functional innovation; these traits allowed stem group onychophorans to exploit a much wider range of lifestyles during the Cambrian than those observed among extant representatives.

The fossil record has previously documented metazoan clades whose extant diversity and disparity reflect only a modest fraction of their earlier evolutionary success (e.g., crinoids, brachiopods), usually resulting from a combination of extrinsic (e.g., environmental) and intrinsic (e.g., developmental) factors (31, 32). Our recognition of a similar pattern affecting total-group Onychophora may be interpreted in light of high rates of genotypic and phenotypic evolution that typify the Cambrian explosion (32, 33), leading to the speciation of luolishaniids and their occupation of a unique paleoecological niche. The causes behind the extinction of the luolishaniid mode of life, although elusive, were likely linked to the evolution of escalating new trophic behaviors associated with the Cambrian radiation. Alternatively, the absence of

luolishaniids in post-Cambrian strata may also reflect the poor fossil record of armored lobopodians (e.g., ref. 34) and restricted distribution of these extinct organisms to sites of exceptional preservation (e.g., ref. 15).

Methods Summary

Digital images for all specimens were captured under bright-field illustration using a Leica DFC 500 digital camera mounted to a Stereoscope Leica M205-C. All images were processed in Adobe Photoshop CS 4. The elemental composition of the dorsal biomineralized spines was analyzed with an FEI XL30 FEGSEM electronic microscope with Oxford instruments using ATM Sili spectrometer and running INCA software.

Phylogenetic Analysis. The data matrix includes 46 taxa and 86 characters (Dataset S1 and SI Appendix, Notes S1 and S2). The analysis was run in TNT (35) under New Technology Search (36, 37). An initial analysis treated all characters as equally weighted; subsequent iterations with variable concavity values (*k*) were used to explore the effect of different degrees of homoplasy penalization to test the robustness of the dataset. Detailed results are provided in SI Appendix, Note S3 and Fig. S8.

Morphospace Analysis. Analyses were based on the phylogenetic dataset (Dataset S1) and used the standard protocol of morphospace studies based on discrete character data (e.g., refs. 38 and 39). Pairwise dissimilarity among taxa was calculated as the mean character difference (e.g., refs. 40 and 41). A principal coordinate analysis was performed on the matrix of morphological dissimilarity to visualize the main features of the onychophoran morphospace (Fig. 5A), but disparity analyses were carried out from the original dissimilarity matrix (SI Appendix, Note S1). Disparity was measured as the mean pairwise dissimilarity (e.g., refs. 41 and 42).

Limb Tagmosis Analysis. Measures of limb complexity were calculated using the coefficient of limb tagmosis proposed by Cisne (43) and based on Brillouin's expression (44):

$$h = \left(\ln N! - \sum_i \ln n_i ! \right) \Big/ N$$

where N is the total number of limb pairs and n the number of limb pairs of the ith type (43, 44); see SI Appendix, Notes S1 and S4 for details.

1. Oliveira IdeS, Read VM, Mayer G (2012) A world checklist of Onychophora (velvet worms), with notes on nomenclature and status of names. *Zookeys* 211(211):1–70.
2. Oliveira IdeS, et al. (2012) Unexplored character diversity in Onychophora (velvet worms): A comparative study of three peripatid species. *PLoS One* 7(12):e51220.
3. Smith MR, Ortega-Hernández J (2014) *Hallucigenia*'s onychophoran-like claws and the case for Tactopoda. *Nature* 514(7522):363–366.
4. Collins D (1986) Paradise revisited. *Rotunda* 19:30–39.
5. Conway Morris S, Robison RA (1988) More soft-bodied animals and algae from the Middle Cambrian of Utah and British Columbia. *Univ Kans Paleontol Contrib* 122:1–48.
6. Ma X, Hou X, Bergström J (2009) Morphology of *Luolishania longicruris* (Lower Cambrian, Chengjiang Lagerstätte, SW China) and the phylogenetic relationships within lobopodians. *Arthropod Struct Dev* 38(4):271–291.
7. García-Bellido DC, Edgecombe GD, Paterson JR, Ma X-Y (2013) A "Collins' monster"-type lobopodian from the Emu Bay Shale Konservat-Lagerstätte (Cambrian), South Australia. *Alcheringa* 37:474–478.
8. Ramsköld L, Chen J-Y (1998) Cambrian lobopodian: Morphology and phylogeny. *Arthropod Fossils and Phylogeny*, ed Edgecombe GD (Columbia Univ Press, New York), pp 107–150.
9. Ortega-Hernández J (2014) Making sense of "lower" and "upper" stem-group Euarthropoda, with comments on the strict use of the name Arthropoda von Siebold, 1848. *Biol Rev Camb Philos Soc*, 10.1111/brv.12168.
10. Yang J, Ortega-Hernández J, Butterfield NJ, Zhang X-g (2013) Specialized appendages in fuxianhuiids and the head organization of early euarthropods. *Nature* 494(7438):468–471.
11. Yang J, Smith MR, Lan T, Hou J-b, Zhang X-g (2014) Articulated Wiwaxia from the Cambrian Stage 3 Xiaoshiba lagerstätte. *Sci Rep* 4:4643.
12. Hou X-G, Bergström J (1995) Cambrian lobopodians—ancestors of extant onychophorans. *Zool J Linn Soc* 114:3–19.
13. Zeng H, Zhao F-C, Yin Z-J, Li G-X, Zhu M-Y (2014) A Chengjiang-type fossil assemblage from the Hongjingshao Formation (Cambrian Stage 3) at Chenggong, Kunming, Yunnan. *Chin Sci Bull* 59:3169–3175.
14. Steiner M, Hu S-X, Liu J-N, Keupp H (2012) A new species of *Hallucigenia* from the Cambrian Stage 4 Wulongqing Formation of Yunnan (South China) and the structure of sclerites in lobopodians. *Bull Geosci* 87:107–124.
15. Caron J-B, Smith MR, Harvey THP (2013) Beyond the Burgess Shale: Cambrian microfossils track the rise and fall of hallucigeniid lobopodians. *Proc Biol Sci* 280(1767):20131613.
16. Butterfield NJ (2002) Leanchoilia guts and the interpretation of three-dimensional structures in Burgess Shale-type fossils. *Paleobiology* 28:155–171.
17. Zhang X-G, Aldridge RJ (2007) Development and diversification of trunk plates of the Lower Cambrian lobopodians. *Palaeontology* 50:401–415.
18. Chen J-Y, Zhou G-Q, Ramsköld L (1995) The Cambrian lobopodian *Microdictyon sinicum* and its broader significance. *Bull Natl Mus Nat Sci* 5:1–93.
19. Ou Q, Shu D, Mayer G (2012) Cambrian lobopodians and extant onychophorans provide new insights into early cephalization in Panarthropoda. *Nat Commun* 3:1261.
20. Liu J-N, Dunlop JA (2014) Cambrian lobopodians: A review of recent progress in our understanding of their morphology and evolution. *Palaeogeogr Palaeoclimatol Palaeoecol* 398:4–15.
21. Hou X-G, Ma X-Y, Zhao J, Bergström J (2004) The lobopodian *Paucipodia inermis* from the Lower Cambrian Chengjiang fauna, Yunnan, China. *Lethaia* 37:235–244.
22. Whittington HB (1978) The lobopod animal *Aysheaia pedunculata* Walcott, Middle Cambrian, Burgess Shale, British Columbia. *Philos Trans R Soc Lond B Biol Sci* 284:165–197.
23. Paterson JR, et al. (2011) Acute vision in the giant Cambrian predator *Anomalocaris* and the origin of compound eyes. *Nature* 480(7376):237–240.
24. Delle Cave L, Simonetta AM (1991) Early Palaeozoic arthropods and problems of arthropod phylogeny: With some notes on taxa of doubtful affinities. *The Early Evolution of Metazoa and the Significance of Problematic Taxa*, eds Simonetta AM, Conway Morris S (Cambridge Univ Press, Cambridge, UK), pp 189–244.
25. Ma X-Y, Edgecombe GD, Legg DA, Hou X-G (2014) The morphology and phylogenetic position of the Cambrian lobopodian *Diania cactiformis*. *J Syst Palaeontology* 12:445–457.
26. Wills MA, Briggs DEG, Fortey RA (1998) Evolutionary correlates of arthropod tagmosis: Scrambled legs. *Arthropod Relationships*, eds Thomas RH, Fortey RA (Springer, Heidelberg), pp 57–65.
27. Daley AC, Edgecombe GD (2014) Morphology of *Anomalocaris canadensis* from the Burgess Shale. *J Paleontol* 88:68–91.
28. Daley AC, Budd GE, Caron J-B, Edgecombe GD, Collins D (2009) The Burgess Shale anomalocaridid *Hurdia* and its significance for early euarthropod evolution. *Science* 323(5921):1597–1600.
29. Vermeij GJ (1994) The evolutionary interaction among species: Selection, escalation, and coevolution. *Annu Rev Ecol Evol Syst* 25:219–236.
30. Eriksson BJ, Tait NN, Budd GE, Janssen R, Akam M (2010) Head patterning and Hox gene expression in an onychophoran and its implications for the arthropod head problem. *Dev Genes Evol* 220(3-4):117–122.
31. Foote M (1999) Morphological diversity in the evolutionary radiation of Paleozoic and post-Paleozoic crinoids. *Paleobiology* 25(suppl1):1–115.
32. Erwin DH (2007) Disparity: Morphological pattern and developmental context. *Palaeontology* 50:57–73.
33. Lee MS, Soubrier J, Edgecombe GD (2013) Rates of phenotypic and genomic evolution during the Cambrian explosion. *Curr Biol* 23(19):1889–1895.
34. Van Roy P, et al. (2010) Ordovician faunas of Burgess Shale type. *Nature* 465(7295):215–218.
35. Goloboff PA, Farris JS, Nixon KC (2008) TNT, a free program for phylogenetic analysis. *Cladistics* 24:415–428.
36. Goloboff PA (1999) Analyzing large datasets in reasonable times: Solutions for composite optima. *Cladistics* 15:415–428.
37. Nixon KC (1999) The parsimony ratchet, a new method for rapid parsimony analysis. *Cladistics* 15:407–414.
38. Brusatte SL, Benton MJ, Ruta M, Lloyd GT (2008) Superiority, competition, and opportunism in the evolutionary radiation of dinosaurs. *Science* 321(5895):1485–1488.
39. Wills MA, Gerber S, Ruta M, Hughes M (2012) The disparity of priapulid, archaeopriapulid and palaeoscolecid worms in the light of new data. *J Evol Biol* 25(10):2056–2076.
40. Sneath PH, Sokal RR (1973) *Numerical Taxonomy* (Freeman, San Francisco).
41. Foote M (1992) Paleozoic record of morphologica diversity in blastozoan echinoderms. *Proc Natl Acad Sci USA* 89(16):7325–7329.
42. Foote MJ (1993) Contributions of individual taxa to overall morphological disparity. *Paleobiology* 19:403–419.
43. Cisne JL (1974) Evolution of world fauna of aquatic free-living arthropods. *Evolution* 28:337–366.
44. Brillouin L (1962) *Science and Information Theory* (Academic, New York), 2nd Ed.

EVOLUTION